$$r = \frac{1}{18}\,\frac{\left(\left(\frac{\chi_{\mathrm{BS}}}{6}\right)^{1/2} + \gamma\right)^2}{\left(N_{\mathrm{A}}\left(\alpha + \frac{1}{\phi_{\mathrm{A}}{}^2}\right)\right)^2}$$

and

$$b_0 = \frac{-\left(\frac{1}{\alpha} + \phi_{\mathrm{A}}{}^2\right)}{N_{\mathrm{A}}{}^2\left(\alpha + \frac{1}{\phi_{\mathrm{A}}{}^2}\right)}$$

References and Notes

(1) Napper, D. H. *Polymeric Stabilization of Colloidal Dispersions*; Academic: London, 1983.

(2) Munch, M. R.; Gast, A. P., preceeding paper in this issue.

(3) *Polymer Adsorption and Dispersion Stability*; Goddard, E. D., Vincent, B., Eds.; American Chemical Society: Washington, DC, 1984.

(4) *The Effect of Polymers on Dispersion Properties*; Tadros, Th. F., Ed.; Academic: London, 1982.

(5) *Adsorption from Solution*; Ottewill, R. H., Rochester, C. H., Smith, A. L., Eds.; Academic: London, 1983.

(6) *Polymer Colloids*; Buscall, R., Corner, T., Stageman, J. F., Eds.; Elsevier Applied Science: London, 1985.

(7) Fleer, G. J.; Scheutjens, J. M. H. M. *Adv. Colloid Interface Sci.* **1982**, *16*, 341.

(8) Hadziioannou, G.; Patel, S.; Granick, S.; Tirrell, M. *J. Am. Chem. Soc.* **1986**, *108*, 2869.

(9) de Gennes, P.-G. *Macromolecules* **1980**, *13*, 1069.

(10) Dolan, A. K.; Edwards, S. F. *Proc. R. Soc. London A* **1974**, *337*, 509.

(11) Alexander, S. *J. Phys. (Les Ulis)* **1977**, *38*, 983.

(12) Noolandi, J.; Hong, K. M. *Macromolecules*, **1982**, *15*, 482; **1983**, *16*, 1443.

(13) Leibler, L.; Orland, H.; Wheeler, J. C. *J. Chem. Phys.* **1983**, *79*, 3550.

(14) Flory, P. *Principles of Polymer Chemistry*; Cornell University: Ithaca, NY, 1953.

(15) Meier, D. J. *J. Polym. Sci., Part C* **1969**, *26*, 81.

(16) Helfand, E.; Tagami, Y. *J. Polym. Sci., Part B* **1971**, *9*, 741.

(17) de Gennes, P.-G. *Macromolecules* **1981**, *14*, 1637.

(18) Israelachvili, Jacob, N. *Intermolecular and Surface Forces*; Academic: London, 1985; Chapter 14.

(19) Pritykin, L. M. *J. Colloid Interface Sci.* **1986**, *112*, 539.

(20) Gast, A. P.; Leibler, L. *Macromolecules* **1986**, *19*, 686.

Surface Interactions in Compatible Polymer (and Block Copolymer) Solutions

Giuseppe Rossi*

Materials Department, University of California, Santa Barbara, California 93106

M. E. Cates

Institute for Theoretical Physics, University of California, Santa Barbara, California 93106.

Received August 3, 1987

ABSTRACT: We study theoretically the effects of competing surface interactions in a system of two miscible polymers (A and B) in a good solvent, using the self-consistent mean-field formulation with ground-state dominance, as is appropriate to moderately concentrated systems. We take the A chains to be attracted to the surface and the B chains to be repelled. From susceptibility arguments, one expects a wide A-rich zone to appear at the surface, close enough to the A–B demixing transition. This (and several other qualitative expectations) is confirmed here by explicit numerical and analytic calculations of (1) concentration profiles and (2) interfacial energies, for various values of the excluded volume parameters and bulk concentrations. Our results are also applicable to the description of A–B block copolymer solutions with competing surface interactions.

1. Introduction

The physics of polymer–surface interactions and polymer adsorption phenomena has been of experimental and theoretical interest for a number of years.[1-11] Recently, particular attention has been paid to the surface properties of multicomponent polymer systems, especially to the structure and energetics of the interface between immiscible simple polymers and/or block copolymers in solutions and blends.[12-17]

In the present work, we extend the study of interfacial properties of multicomponent polymer systems in a somewhat different direction. Our concern is with the system polymer A + polymer B + good solvent (with A and B compatible) interacting with a boundary surface that is attractive to one polymer species (A) but repulsive to the other (B). This situation can presumably be realized experimentally, although we known of no example involving the mica surfaces that so far have ordinarily been used for this type of experiment.[10-11,14-15] We will presume the bulk concentrations of the two species to be high enough that mean-field theory is applicable and, moreover, that the surface interactions are of such a strength that the assumption of "ground-state dominance"[18] is appropriate for both polymer species. (For a comprehensive review of these ideas, see ref 4.)

As will become clear, under these conditions, much of the physics is controlled by the A–B excluded volume interaction, w_{AB}. For example, if this is zero, the A and B profiles are just those given in ref 3 for independent systems of attracted (A) and repelled (B) polymers. Whenever the coupling w_{AB} is nonzero, however, new effects arise, in both the interfacial energy and the concentration profiles of the two species. For example, when this coupling is strongly enough repulsive that the bulk A–B mixture is close to phase separation, the surface interaction can induce a strong local segregation, and the concentration profiles of A and B are extremely different from those that each polymer would have in the absence of the other.

While our discussion is phrased in terms of a mixed solution of A and B chains, it is notable that given our assumption of ground-state dominance, the computed profiles also apply (under appropriate conditions of con-

0024-9297/88/2221-1372$01.50/0 © 1988 American Chemical Society

centration) to the case of A–B block copolymers with selective surface interactions. (This is shown in section 3.) Some experiments on these systems are reported in ref 14 and 15. So far, the experiments have been restricted to conditions when the bulk chain concentration of the A–B block is very small. Our work, however, concerns the opposite regime, in which the behavior of the block reduces to that of a simple A–B mixture.

2. Self-Consistent Equations for Concentration Profiles

We start by recalling the self-consistent equation[1,4,18] for the ground-state "wave function" $\psi(z)$ appropriate to a polymer solution in an external potential $V(z)$, which is a function of the one-dimensional coordinate z:

$$-\frac{a^2}{6}\frac{\partial^2\psi(z)}{\partial z^2} + V\psi(z) + w\phi(z)\,\psi(z) = \epsilon\psi(z) \qquad (1)$$

Here a is a monomeric length, w is the excluded volume parameter, and the concentration $\phi(z)$ obeys

$$\phi(z) = |\psi(z)|^2 \qquad (2)$$

The eigenvalue ϵ is fixed by imposing the boundary condition $\phi(z) \rightarrow c$, at $z \rightarrow +\infty$; here c is the value of the bulk concentration.

For the case when $V(z)$ represents an impenetrable wall (at $z = 0$, say) with a localized surface interaction, it is possible formally to set $V = 0$ in (1), while retaining the effect of the potential through the boundary condition[4]

$$\left.\frac{1}{\psi}\frac{\mathrm{d}\psi}{\mathrm{d}z}\right|_{z=0} = \kappa \qquad (3)$$

where κ is a parameter (with dimension of 1/length) that is negative for an attractive surface while for a purely repulsive wall, $\kappa \rightarrow +\infty$, which ensures from (3) that $\psi(0) \rightarrow 0$.

Under these conditions and with $\psi = c^{1/2}f$, (1) becomes

$$\partial_x{}^2 f = 2(f^3 - f) \qquad (4)$$

where $x = z/\xi_E$ and $\xi_E = a/(3cw)^{1/2}$ is the Edwards correlation length. The interfacial energy γ can be written as

$$\frac{\gamma - \gamma_0}{T} = \frac{\xi_E w c^2}{2}\left(-\kappa\xi_E f_s{}^2 + \int_0^\infty (\partial_x f)^2 + (f^2 - 1)^2\,\mathrm{d}x\right) \qquad (5)$$

where γ_0 is the interfacial energy of the pure solvent and f_s is the value of $f(x)$ at the wall. The energy difference is negative for attractive and positive for repulsive walls. Note that (3) and (4) can be obtained minimizing (5) with respect to f_s and $f(x)$.

As discussed in ref 1, 4, and 18, (1–5) provide an adequate description of the concentration profile and free energy of polymers, at an adsorbing or repelling surface, under two general conditions: (1) the concentration of the bulk solution is high enough (and/or that the solution is close enough to Θ conditions) for mean-field averaging to be applicable; (2) the characteristic length scale for the decay of the concentration profile, toward its bulk value, is small compared to the radius of gyration of a single chain in solution. When condition 2 holds, the concentration profile and interfacial free energy for chains of finite length approach what they would be for a system of infinitely long chains (at the same monomer concentration, in bulk). Since all monomers become equivalent in this limit, it is no longer necessary to keep separate track of the spatial densities associated with different monomer positions in the chemical sequence. Correspondingly, only a single "order parameter", $\psi(z)$, needs to be considered. The calculation of $\psi(z)$ amounts to finding the ground-state wave function of the self-consistent Schroedinger equation (1); hence the term ground-state dominance is used to denote situations in which such a treatment is appropriate.

The modifications required to (1–5) are rather straightforward to describe a mixed polymer solution under similar conditions. Each component (A or B) is described by a separate wave function; these obey[19]

$$-\frac{a^2}{6}\frac{\partial^2\psi_A(z)}{\partial z^2} + V_A\psi_A(z) + [w_{AA}\phi_A(z) + w_{AB}\phi_B(z)]\,\psi_A(z) = \epsilon_A\psi_A(z) \qquad (6a)$$

$$-\frac{a^2}{6}\frac{\partial^2\psi_B(z)}{\partial z^2} + V_B\psi_B(z) + [w_{BB}\phi_B(z) + w_{AB}\phi_A(z)]\,\psi_B(z) = \epsilon_B\psi_B(z) \qquad (6b)$$

The local concentrations are

$$\phi_A(z) = |\psi_A(z)|^2 \qquad (7a)$$

$$\phi_B(z) = |\psi_B(z)|^2 \qquad (7b)$$

The eigenvalues ϵ_A and ϵ_B are fixed by requiring that at $z \rightarrow +\infty$ the concentrations $\phi_A(x)$ and $\phi_B(x)$ reach their bulk values, c_A and c_B, respectively. In the above equations, we have omitted terms corresponding to the entropy of mixing of the two species. This is appropriate in the limit of long chains. (Formally, these terms are of the same order as those already omitted in the ground-state dominance treatment.)

For each species A and B it is again possible to replace the short-range surface potentials V_A and V_B by a boundary condition as in (3); from now on we shall take V_A attractive and V_B repulsive so that the corresponding parameters κ_A and κ_B are respectively negative and positive. We will be mainly interested in the case when κ_A is finite (finite surface attraction) and $\kappa_B \rightarrow \infty$ (perfect repulsion from the surface).

Setting $\psi_A(z) = (c_A)^{1/2}f_A$ and $\psi_B(z) = (c_B)^{1/2}f_B$, (6a) and (6b) can be rewritten as

$$\partial_x{}^2 f_A = 2((1 - \eta_A)f_A{}^2 + \eta_A f_B{}^2)f_A - 2f_A \qquad (8a)$$

$$\delta\partial_x{}^2 f_B = 2(\eta_B f_A{}^2 + (1 - \eta_B)f_B{}^2)f_B - 2f_B \qquad (8b)$$

where we have defined

$$\eta_A = w_{AB}c_B/\epsilon_A \qquad (9a)$$

$$\eta_B = w_{AB}c_A/\epsilon_B \qquad (9b)$$

$$\epsilon_A = w_{AA}c_A + w_{AB}c_B \qquad (10a)$$

$$\epsilon_B = w_{AB}c_A + w_{BB}c_B \qquad (10b)$$

$$\xi_A = a/(3\epsilon_A)^{1/2} \qquad (11a)$$

$$\xi_B = a/(3\epsilon_B)^{1/2} \qquad (11b)$$

$$\delta = \xi_B{}^2/\xi_A{}^2 \qquad (12)$$

In (8a) and (8b) we have chosen ξ_A as our unit of length (i.e., $x = z/\xi_A$), so the equations depend only on three independent bulk parameters, η_A, η_B, and δ.[20] We discuss the solution of the equations for various values of these parameters in section 4.

In terms of these parameters the interfacial tension in the presence of both species can be written as

$$\frac{\gamma - \gamma_0}{T} = \frac{\xi_A\epsilon_A c_A}{2}\left[(\kappa_A\xi_A)f_{As}{}^2 + \left(\kappa_B\frac{\xi_A\eta_A\delta}{\eta_B}\right)f_{Bs}{}^2 + \int_0^\infty (\partial_x f_A)^2 + \frac{\eta_A\delta}{\eta_B}(\partial_x f_B)^2 + (1 - \eta_A)(f_A{}^2 - 1)^2 + \frac{\eta_A}{\eta_B}(1 - \eta_B)(f_B{}^2 - 1)^2 + 2\eta_A(f_A{}^2 - 1)(f_B{}^2 - 1)\,\mathrm{d}x\right] \qquad (13)$$

Note that the only coupling between (8a) and (8b) is through the mutual excluded volume, w_{AB}. For $w_{AB} = 0$ the two equations are decoupled, so the two polymer species behave independently. In this case exact solutions can be given; they are[3]

$$f_A{}^0 = \coth\left(\frac{z + z_{0A}}{\xi_A{}^0}\right) \qquad (14a)$$

$$f_B{}^0 = \tanh\left(\frac{z + z_{0B}}{\xi_B{}^0}\right) \qquad (14b)$$

where the boundary condition at the surface are used to determine the integration constants z_{0A} and z_{0B} and we have used the notation $\xi_A{}^0 = \xi_A(w_{AB} = 0)$ and $\xi_B{}^0 = \xi_B(w_{AB} = 0)$.

For the polymer solution described by (8a) and (8b) phase separation in the bulk occurs for[21]

$$w_{AB}{}^2 > w_{AA}w_{BB} \qquad (15)$$

Correspondingly our equations become unstable[22] in the limit $w_{AB} \geq (w_{AA}w_{BB})^{1/2}$. The solution of the equations as this limit is approached is among those discussed in section 4.

3. Block Copolymer Solutions

Consider again a single species of chain. In the limit of high molecular weight, the propagator $G(s,s';z,z')$, which denotes[1,4] the statistical weight for configurations in which monomers s and s' on the chain occupy spatial positions z and z', respectively, depends on s and s' only through $n \equiv |s - s'|$. Under conditions of ground-state dominance, it is factorable over spatial positions, as follows:

$$G(s,s';z,z') = G_n(z,z') \propto \psi(z)\, \psi(z')\, \exp(-\epsilon n) \qquad (16)$$

Here $\psi(z)$ is the ground-state wave function obeying (1), and ϵ is the corresponding eigenvalue. The partition function per chain is simply

$$Z = \int \mathrm{d}z\, \mathrm{d}z'\, G_M(z,z') = \bar{\psi}^2 \exp(-\epsilon M) \qquad (17)$$

where M is the chain length and $\bar{\psi} \equiv \int \mathrm{d}z\, \psi(z)$.

For a diblock copolymer, containing M_A monomers of type A and M_B of type B, we should distinguish three different propagators $G_n^A(z,z')$, $G_n^B(z,z')$, and $G_{n,m}^{AB}(z,z')$. The first of these is the weight for configurations in which two monomers of species A, a distance n apart in the chemical sequence, are at positions z and z'; the second describes a similar quantity for monomers of species B. The third propagator, $G_{n,m}^{AB}(z,z')$, is the weight for a monomer of type A, located on the chain n monomers from the A–B junction point, to be at spatial position z, while a monomer of type B, m monomers from the junction on the opposite site, is at z'.

Assuming ground-state dominance for both components A and B, we write

$$G_n^A(z,z') \propto \psi_A(z)\, \psi_A(z')\, \exp(-\epsilon_A n) \qquad (18a)$$

$$G_n^B(z,z') \propto \psi_B(z)\, \psi_B(z')\, \exp(-\epsilon_B n) \qquad (18b)$$

$$G_{n,m}^{AB}(z,z') = \int \mathrm{d}z''\, G^A{}_n(z,z'')\, G^B{}_m(z'',z') \propto \langle\psi_A|\psi_B\rangle\, \psi_A(z)\, \psi_B(z')\, \exp(-\epsilon_A n - \epsilon_B m) \qquad (18c)$$

where

$$\langle\psi_A|\psi_B\rangle \equiv \int \mathrm{d}z\, \psi_A(z)\, \psi_B(z)$$

The partition function per chain is now

$$Z = \int \mathrm{d}z\, \mathrm{d}z'\, G_{M_A,M_B}^{AB}(z,z') \propto \langle\psi_A|\psi_B\rangle \bar{\psi}_A\bar{\psi}_B \exp(-\epsilon_A M_A - \epsilon_B M_B) \qquad (19a)$$

where $\bar{\psi}_A = \int \mathrm{d}z\, \psi_A(z)$ and $\bar{\psi}_B = \int \mathrm{d}z\, \psi_B(z)$. More precisely, (19a) may be rewritten in the form

$$Z = \frac{\langle\psi_A|\psi_B\rangle}{\bar{\psi}_A\bar{\psi}_B} Z_{\text{mix}} \qquad (19b)$$

where Z_{mix} denotes the partition function (per pair of chains) of a mixture of equal numbers of chains of the two species rather than that of diblocks. Since the extra factor Z/Z_{mix} is independent of chain length, when we take the logarithm of Z to obtain a free energy, this factor will give a term that is negligible compared to those linear in M_A and M_B: $\log Z = \log (Z_{\text{mix}}) + \mathcal{O}(1) \simeq \epsilon_A M_A + \epsilon_B M_B + \mathcal{O}(1)$. Thus the free energy of the *diblock* system, as a functional of the wave functions ψ_A and ψ_B, may be taken as identical with that of the corresponding *mixture*, at this level of approximation. It follows that the equilibrium concentration profiles and interfacial energies will themselves be the same for the diblock as for the mixture.

This result may be understood physically by recalling that the ground-state dominance calculation for a mixture is valid only if the characteristic length scales of the interfacial profiles are much smaller than the gyration radii of the corresponding chains (see section 2). On the other hand, the distinction between a mixture of chains and the corresponding system of diblocks is only manifested on scales comparable to the radius of a block or chain. Thus one indeed expects the two systems to be equivalent with regard to interfacial profiles and energies. It is clear, moreover, that block copolymers of any other geometry (triblock, star, etc.) are also equivalent to mixtures, for the purposes of this treatment.

4. Solutions of the Equations

Equations 8a,b were solved numerically by relaxation methods for various values of the excluded volume parameters and bulk concentrations. Solutions were also found analytically in some limiting cases. In section 4.1, we give detailed results for the case when the bulk concentrations and self-excluded volume parameters are equal for the two species. (This leaves w_{AB} as the single controlling variable.) The results for $w_{AA} \neq w_{BB}$ and/or $c_A \neq c_B$ are qualitatively similar and are described more briefly in sections 4.2 and 4.3.

4.1 $\boldsymbol{w_{AA} = w_{BB}}$ and $\boldsymbol{c_A = c_B = c}$.

In this case the equations can be rewritten as

$$\partial_x{}^2 f_A = ((2 - \zeta)f_A{}^2 + \zeta f_B{}^2 - 2)f_A \qquad (20a)$$

$$\partial_x{}^2 f_B = (\zeta f_A{}^2 + (2 - \zeta)f_B{}^2 - 2)f_B \qquad (20b)$$

which involve the single independent parameter

$$\zeta = 2w_{AB}/(w_{AA} + w_{AB}) \qquad (21)$$

One can define the Edwards length $\xi_E(\zeta) = \xi_A = \xi_B$ so that $x = z/\xi_E$.

For w_{AB} positive, $\zeta \rightarrow 1$ corresponds to the limit of miscibility. As ζ is increased from 0 to 1, polymer B (which is subject to a repulsive potential) is progressively expelled away from a wider and wider zone near the wall; polymer A moves in to fill the region depleted of species B. This situation is illustrated in Figures 1 and 2, which show the evolution of the concentration profiles with ζ when B experiences perfect repulsion while A is subject to weak (Figure 1) and moderately strong (Figure 2) attraction (note that the total concentration of polymer close to the surface increases with ζ). For $\zeta \rightarrow 1$, the two species be-

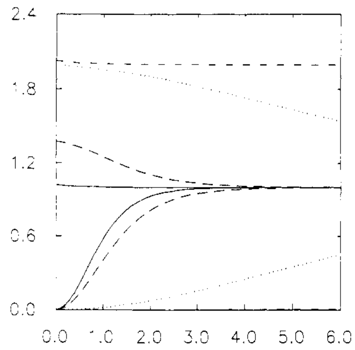

Figure 1. Case $w_{AA} = w_{BB}$, $c = c_A = c_B$. Concentration profiles $\phi_A(x)$ (upper curves) and $\phi_B(x)$ (lower curves) in units of c. Here B experiences perfect repulsion and (see ref 20) $\kappa_A{}^0 = -0.02$ (weak attraction for A). The curves correspond to $\zeta = 0$ (continuous line), $\zeta = 0.6$ (dashed line), $\zeta = 0.99$ (dotted line), and $\zeta = 0.9999$ (dash dotted line); note that in this latter case $\phi_B(x) \approx 0$.

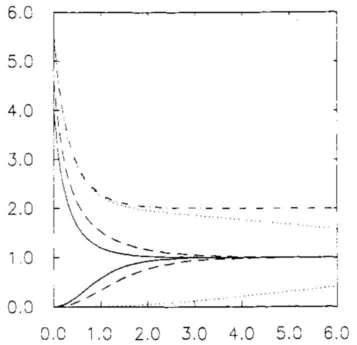

Figure 2. Same as in Figure 1 but with $\kappa_A{}^0 = -1.5$ (moderately strong attraction for A).

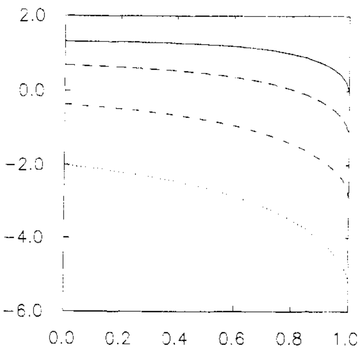

Figure 3. Interfacial energy $(\gamma - \gamma_0)$ measured in units of $(Tw_{AA}c^2\xi_E(\zeta{=}0))/2$ as a function of ζ when species B is subject to perfect repulsion. The curves correspond to $\kappa_A{}^0 = -0.02$ (continuous line), $\kappa_A{}^0 = -0.5$ (dashed line), $\kappa_A{}^0 = -1$ (dashed dotted line), and $\kappa_A{}^0 = -1.5$ (dotted line).

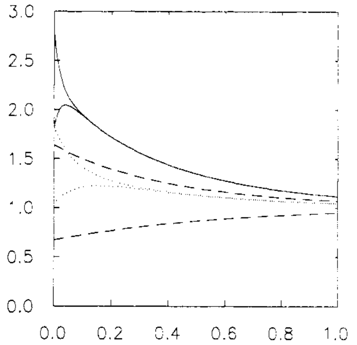

Figure 4. Case $w_{AA} = w_{BB}$, $c = c_A = c_B$. Concentration profiles $\phi_A(x)$ (upper curves) and $\phi_B(x)$ (lower curves) in units of c. Here $\kappa_A{}^0 = -0.5$ and $\kappa_B{}^0 = 0.4$. The curves correspond to $\zeta = 0$ (dashed line), $\zeta = -16$ (dotted line), and $\zeta = -256$ (continuous line).

come indistinguishable insofar as excluded volume interaction is concerned; the presence of the wall then induces a phase separation where all of the polymer B is pushed further away from the wall than all of polymer A. Close to the surface, the profile of species A is simply what it would be in absence of B, but for a bulk concentration equal to $2c$. This corresponds to the formal limiting solutions

$$f_A(x) \to 2^{1/2} \coth (x + x_{1A}) \qquad f_B(x) \to 0 \tag{22}$$

(where $x_{1A} = {}^1/_2 \sinh^{-1} (2/|\kappa_A\xi_E(\zeta{=}1)|)$). Indeed, in both Figures 1 and 2, the profile corresponding to $\zeta = 0.9999$ nearly coincides with this solution. One can define the characteristic lengths L_A and L_B where

$$L_A = \xi_E \int_0^\infty |f_A{}^2 - 1| \,\mathrm{d}x \tag{23}$$

with a similar expression for L_B; these lengths measure the distance over which the effect of the surface potential is felt within the bulk. It is found numerically that as $\epsilon = (1 - \zeta) \to 0$ these lengths diverge as $\epsilon^{-1/2}$. This is, of course, the power expected from a mean-field calculation: recall that in mean-field theory, the susceptibility of the mixture diverges as $\epsilon^{-1/2}$ as the demixing point is approached.[4]

Since the effect of the attractive potential increases with w_{AB}, the interfacial free energy is a decreasing function of ζ; in the limit $\epsilon \to 0$ it reaches the value corresponding to (22); i.e., for a perfectly repulsive potential

$$\frac{\gamma - \gamma_0}{T} = \frac{\xi_E \epsilon_A c}{3}[4 - 3 \coth (x_{1A}) - \coth^3 (x_{1A})] \tag{24}$$

This is indeed confirmed by a numerical evaluation using the computed profiles in conjunction with (13). Figure 3 shows the behavior of the interfacial tension as a function of ζ for different values of the attraction parameter κ_A. For $\zeta \to 1$ this quantity is negative for any $\kappa_A < 0$, and it is finite as should be expected of surface properties in correspondence to singularities of bulk parameters.

While the situation with w_{AB} positive is easier to realize physically, the case w_{AB} negative (a net attraction between the two polymer species) may also be of some interest. The limit of solubility ($w_{AB} \to -w_{AA}$) corresponds to $\zeta \to -\infty$. (For a stronger attraction than this, precipitation of a highly concentrated A–B mixture will occur.) In this limit the Edwards length diverges as $|\zeta|^{1/2}$. As ζ decreases from 0 to $-\infty$, the profiles f_A and f_B tend to coincide everywhere except in a region immediately adjacent to the wall, whose width is of order $\xi_E{}^0 = \xi_E(\zeta{=}0)$. This behavior is shown in Figures 4 and 5. Note that in the region where the two profiles coincide they have the form of (14); i.e., the two components behave as a single species that can experience either a net attraction (Figure 4) or a net repulsion (Figure 5) from the interface.

4.2 $w_{AA} \neq w_{BB}$ and $c_A = c_B = c$. In this case $\delta = \eta_B/\eta_A$ so that there are only two independent parameters. As w_{AB} is increased from 0 to the miscibility limit $w_{AB} \to (w_{AA}w_{BB})^{1/2}$ (i.e., $(\eta_A + \eta_B) \to 1$), the qualitative behavior of the system is similar to that discussed in section 4.1: species A displaces species B from an increasingly wider region close to the wall. The formal limiting solution for $\epsilon = (1 - \eta_A + \eta_B) \to 0$ is

$$f_A(x) \to \frac{1}{(1 - \eta_A)^{1/2}} \coth (x + x_{1A}) \qquad f_B(x) \to 0 \tag{25}$$

(where $x_{1A} = {}^1/_2 \sinh^{-1} (2/|\kappa_A\xi_A(\epsilon{=}0)|)$). Due to the difference in self-interaction parameters the bulk polymer concentration corresponding to this solution is different from the total concentration $2c$ at $w_{AB} = 0$. It is smaller than $2c$ if $w_{BB} < w_{AA}$, larger otherwise. The profiles shown

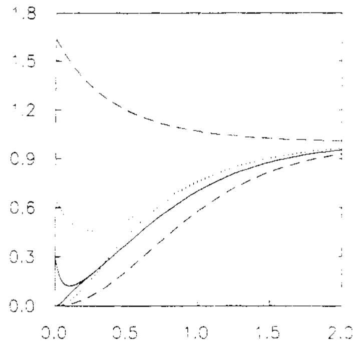

Figure 5. Case $w_{AA} = w_{BB}$, $c = c_A = c_B$. Concentration profiles $\phi_A(x)$ (upper curves) and $\phi_B(x)$ (lower curves) in units of c. Here B experiences perfect repulsion, and $\kappa_A{}^0 = -0.5$. The curves correspond to $\zeta = 0$ (dashed line), $\zeta = -16$ (dotted line), and $\zeta = -1024$ (continuous line).

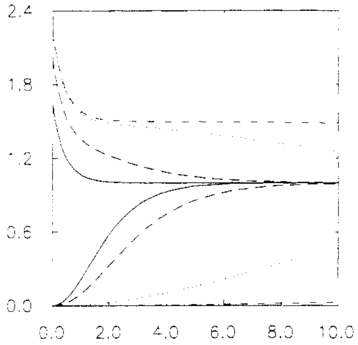

Figure 6. Case $w_{AA} \neq w_{BB}$, $c = c_A = c_B$. Concentration profiles $\phi_A(x)$ (upper curves) and $\phi_B(x)$ (lower curves) in units of c. Here $w_{BB} = w_{AA}/4$; B experiences perfect repulsion, and $\kappa_A{}^0 = -0.5$. The curves correspond to $\epsilon = 1$ (continuous line), $\epsilon = 0.2$ (dashed line), $\epsilon = 0.01$ (dotted line), and $\epsilon = 0.0004$ (dash dotted line).

in Figure 6 refer to the first situation. One can define characteristic lengths L_A and L_B in analogy to (23): as expected they diverge as $\epsilon^{-1/2}$ as the limit of miscibility is approached.

4.3 $w_{AA} = w_{BB}$ and $c_A \neq c_B$. Again the situation is not qualitatively different from the corresponding one discussed in section 4.1: as $\zeta' = w_{AB}/w_{AA}$ is increased from 0 up to the miscibility limit ($\zeta' \rightarrow 1$), polymer B is expelled away from the wall. The limiting solutions for $\zeta' \rightarrow 1$ are

$$f_A(x) \rightarrow \left(\frac{(c_A + c_B)}{c_A}\right)^{1/2} \coth\,(x + x_{1A}) \qquad f_B(x) \rightarrow 0 \tag{26}$$

(where $x_{1A} = {}^1/_2 \sinh^{-1}(2/|\kappa_A \xi_A(\zeta'{=}1)|)$). Note that in this case since $w_{AA} = w_{BB}$ the total bulk concentration in the miscibility limit is the same as the bulk concentration for $w_{AB} = 0$. The case $c_A < c_B$ is illustrated in Figure 7: as w_{AB} increases the concentration of A close to the wall becomes larger than that of B; it reaches a bulk value ($c_A + c_B$) in the limit of miscibility (dash dotted line). Again, it is found numerically that the characteristic lengths L_A and L_B diverge with the expected mean-field theory behavior $(1 - \zeta')^{-1/2}$.

5. Discussion

The calculations presented above are expected to be valid for moderately concentrated systems of long chains, for which the assumptions of mean-field theory and ground-state dominance are appropriate. The latter requires that the characteristic lengths L_A and L_B are small compared to a chain radius, and clearly this breaks down close enough to the phase separation ($\zeta \rightarrow 1$) at which the interfacial thickness diverges. Similarly, the distinction between mixed solutions and block copolymer solutions will become important near this point. Nonetheless, the calculations presented here have confirmed explicitly a number of qualitative expectations for the density profiles and interfacial energies of such systems in the presence of competing interactions.

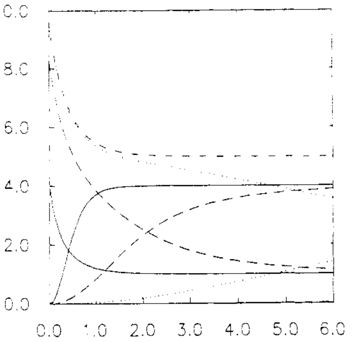

Figure 7. Case $w_{AA} = w_{BB}$, $c_A \neq c_B$. Concentration profiles $\phi_A(x)$ (decreasing curves) and $\phi_B(x)$ (increasing curves) in units of c_A. Here $c_B = 4c_A$; B experiences perfect repulsion, and $\kappa_A{}^0 = -0.5$. The curves correspond to $\zeta' = 0$ (continuous line), $\zeta' = 0.8$ (dashed line), $\zeta' = 0.99$ (dotted line), and $\zeta' = 0.9999$ (dash dotted line).

Specifically, it was seen that the difference between the concentration profiles of the mixture and those of separate solutions of the two species depended principally on the mutual excluded volume parameter w_{AB}. When this parameter is small, the two profiles are essentially superposed. For positive values of w_{AB}, the attracted species (A) partially displaces the repelled one (B) in a region near the surface, the width of this region diverging with the usual mean-field exponent as the point of bulk-phase separation is approached. The interfacial energy increment remains finite and depending on the interaction parameters and bulk concentrations can be positive or negative. Close enough to demixing, however, it is always negative, since the attracted species benefits from the presence of the surface while the repelled one can be displaced from the surface region with only a small free-energy cost. One the other hand, when w_{AB} is negative, the two profiles approach one another, and except for a layer immediately adjacent to the wall the system eventually behaves as a single species with an averaged surface interaction. While similar effects may be expected[2] in A–B blends of pure polymer (with no solvent present), there will be significant differences due to the constraint on the total density ($\phi_A + \phi_B = 1$), which is absent from the systems considered here. Indeed, the numerical results indicate a total chain density that departs strongly from a constant value, in the interfacial region.

Acknowledgment. We thank Daniel Hone and Phil Pincus for many useful discussions and comments. This work was funded in part by the Department of Energy under Grant No. DE-FG03-87ER45288 and by the National Science Foundation under Grant No. PHY82-17853, supplemented by funds from NASA.

References and Notes

(1) de Gennes, P.-G. *Rep. Prog. Phys.* **1969**, *32*, 187. Edwards, S. F. *Proc. Phys. Soc., London* **1966**, *88*, 265.
(2) Roe, R. J. *J. Chem. Phys.* **1974**, *60*, 4192.
(3) Jones, I. S.; Richmond, P. *J. Chem. Soc., Faraday Trans. 2* **1977**, *73*, 1062.
(4) de Gennes, P.-G. *Scaling Concepts in Polymer Physics*; Cornell University Press: Ithaca, NY, 1979.
(5) de Gennes, P.-G. *Macromolecules* **1981**, *14*, 1637; **1982**, *15*, 492.
(6) Fleer, G. J.; Scheutjens, J. M. H. M. *Adv. Colloid Interface Sci.* **1982**, *16*, 341.
(7) Eisenriegler, E.; Kremer, K.; Binder, K. *J. Chem. Phys.* **1982**, *77*, 6296.

(8) Ober, R.; Paz, L.; Taupin, C.; Pincus, P.; Boileau, S. *Macromolecules* **1983**, *16*, 50.

(9) Di Meglio, J. M.; Ober, R.; Paz, L.; Taupin, C.; Pincus, P.; Boileau, S. *J. Phys.* (*Les Ulis, Fr.*) **1983**, *44*, 1035.

(10) Israelachvili, J. N.; Tandon, R. K.; White, L. R. *Nature* (*London*) **1979**, *277*, 120. Klein, J. *Nature* (*London*) **1980**, *288*, 248.

(11) Israelachvili, J. N.; Tirrel, M.; Klein, J.; Almog, Y. *Macromolecules* **1984**, *17*, 205. Klein, J.; Almog, Y. *J. Colloid Interface Sci.* **1985**, *106*, 33.

(12) Poser, C. I.; Sanchez, I. C. *Macromolecules* **1981**, *14*, 361.

(13) Leibler, L. *Macromolecules* **1982**, *15*, 1283.

(14) Hadziioannou, G.; Patel, S.; Granick, S.; Tirrell, M. *J. Am. Chem. Soc.* **1986**, *108*, 2869.

(15) Granick, S.; Patel, S.; Tirrell, M. *J. Chem. Phys.* **1986**, *85*, 5370.

(16) Fredrickson, G. H. *Macromolecules* **1987**, *20*, 2535.

(17) Marques, C. M.; Joanny, J. F.; Leibler, L., preprint, 1987.

(18) Moore, M. A. *J. Phys. A: Math. Gen.* **1977**, *10*, 305.

(19) The relation between the effective excluded volume parameters w_{AA}, w_{BB}, and w_{AB} and the Flory parameters is as follows: Let Φ_A, Φ_B, and Φ_S be the volume fractions of polymer A, polymer B, and solvent, respectively. The Flory–Huggins free-energy form $F = F_{mix} + F_{int}$, where (in the long chain limit) $F_{mix} = T\Phi_S \ln \Phi_S$ and

$$F_{int}/T = \tfrac{1}{2}\sum_{ij}\chi_{ij}^{dir}\Phi_i\Phi_j$$

Expanding to quadratic order in Φ_A and Φ_B (and using $\sum_i\Phi_i = 1$), we obtain

$$F/T = \tfrac{1}{2}(\Phi_A + \Phi_B)^2 - \sum_{ij}\chi_{ij}\Phi_i\Phi_j$$

where the sum is over species A and B only. The resulting Flory-type parameters obey

$$\chi_{AA} = \chi_{AS}^{dir} - (\chi_{AA}^{dir} + \chi_{SS}^{dir})/2$$

$$\chi_{BB} = \chi_{BS}^{dir} - (\chi_{BB}^{dir} + \chi_{SS}^{dir})/2$$

$$\chi_{AB} = (\chi_{AS}^{dir} + \chi_{BS}^{dir} - \chi_{AB}^{dir} - \chi_{SX}^{dir})/2$$

On the other hand, in terms of the excluded volume parameters, F is written as

$$F/T = \tfrac{1}{2}\sum_{ij}w_{ij}\Phi_i\Phi_j$$

Hence the excluded volume parameters are related to the Flory χ parameters as follows:

$$w_{AA} = 1 - 2\chi_{AS}$$

$$w_{BB} = 1 - 2\chi_{BS}$$

$$w_{AB} = 1 - 2\chi_{AB}$$

(20) Note that the unit of length ξ_A does depend on these parameters. On the other hand, the surface potential experienced by the polymer is independent of the bulk parameters. Therefore, we introduce the dimensionless surface parameters $\kappa_A{}^0 = \xi_A{}^0\kappa_A$ and $\kappa_B{}^0 = \xi_A{}^0\kappa_B$; we ask that the logarithmic derivative of f_A and f_B with respect to x be equal to $(\xi_A/\xi_A{}^0)\kappa_A{}^0$ and $(\xi_A/\xi_A{}^0)\kappa_B{}^0$, respectively.

(21) Under the assumption that the free energy is dominated by two-body repulsions, the bulk free energy per unit volume for the mixture is

$$f_{mix} = (w_{AA}c_A{}^2 + w_{BB}c_B{}^2 + 2w_{AB}c_Ac_B)/2$$

while for a phase-separated state

$$f_{ps} = (w_{AA}c_A{}^2 + w_{BB}c_B{}^2 + 2(w_{AA}w_{BB})^{1/2}c_Ac_B)/2$$

from which (15) follows immediately.

(22) We are indebted to Prof. Daniel W. Hone for illuminating comments on this point.

Interphase Composition Profile in SB/SBS Block Copolymers, Measured with Electron Microscopy, and Microstructural Implications

Richard J. Spontak and Michael C. Williams*

Center for Advanced Materials, Lawrence Berkeley Laboratory, and Department of Chemical Engineering, University of California, Berkeley, California 94720-9989

David A. Agard

Department of Biochemistry and Biophysics, University of California, San Francisco, California 94143-0448.

Received May 4, 1987;
Revised Manuscript Received September 4, 1987

ABSTRACT: The behavior of microphase-separated block copolymers has major contributions from the mixed interphase existing between the two homogeneous phases. However, relatively little has been known about the interphase itself and, in particular, its composition profile has never been measured directly. Here, we have used quantitative transmission electron microscopy to acquire the shape of the volume-fraction composition profile across this interphase. Measurements were made on four styrene (S)/butadiene (B) block copolymers having structure SBS (three) and SB (one), with molecular weights 1.0–2.3 × 10^5 g/mol and overall volume compositions of 0.24–0.38 styrene. Results, averaged over the four samples, depict an asymmetric interphase profile, being rich in styrene (54 vol %) in agreement with new differential scanning calorimetry data and with dynamic mechanical testing studies of others. This profile is then used in an equilibrium thermodynamic theory (which extends earlier work by adding an enthalpic "Debye" term that accounts for molecular interactions beyond nearest neighbors) to predict various microstructural and thermal properties of the bulk polymer. Excellent agreement with reported data is obtained for the predicted interphase thickness and interphase volume fraction and for predictions of the repeat distance for lamellar SB copolymers.

Introduction

Block copolymers are known to undergo microphase separation under certain conditions (normally encountered in practice) of composition, molecular weight, temperature, and molecular architecture. The result of this microphase separation is the formation of either a cocontinuous composite of lamellar elements or a dispersed phase of domains distributed in a continuous matrix (Figure 1). Since these microphase-separated block copolymers exhibit thermal and mechanical properties unlike those of either homopolymer or a random copolymer of similar composition,

---

* To whom correspondence should be addressed.

0024-9297/88/2221-1377$01.50/0